Fabrication of Standalone Cell-laden Collagen Vascular Network Scaffolds Using Fugitive Pattern-Based Printing-then-Casting Approach

Yifei Jin[1], *Wenxuan Chai*[1], *Yong Huang*[1,2,3,]*

[1]Department of Mechanical and Aerospace Engineering, University of Florida, Gainesville, FL 32611, USA.

[2]Department of Materials Science and Engineering, University of Florida, Gainesville, FL 32611, USA.

[3]Department of Biomedical Engineering, University of Florida, Gainesville, FL 32611, USA.

*Corresponding author, Department of Mechanical and Aerospace Engineering, University of Florida, Gainesville, FL 32611, USA

Phone: 001-352-392-5520, Fax: 001- 352-392-7303, Email: yongh@ufl.edu.

KEYWORDS: standalone; collagen; living cells; vascular network scaffolds; fugitive vascular tree pattern; printing-then-casting

ABSTRACT

Vascular networks are of great significance in tissue engineering and viewed as the first step to fabricate human tissues. While various techniques have been investigated to create vascular and vascular-like networks, the fabrication of standalone pure collagen-based vascular constructs is still a challenge due to the poor extrudability, weak mechanical property, and long cross-

linking time of pure collagen solutions. In this study, a fugitive pattern-based printing-then-casting approach is investigated. The proposed alginate-based fugitive ink has the excellent mechanical strength (by adding Laponite), printability (by adding Laponite nanoclay), and controllable gelation rate (by adding disodium hydrogen phosphate). Using this fugitive ink, complex vascular-like structures can be easily printed and cross-linked in Laponite EP bath as fugitive vascular tree patterns. Each fugitive vascular tree pattern is then embedded in a gelatin baths to make a gelatin mold with the tree patterns. With the help of sodium citrate, the fugitive vascular tree-pattern is liquefied and removed to create the gelatin mold with vascular channels. Finally, a standalone collagen vascular network scaffold embedded with fibroblasts can be fabricated by casting cell-laden collagen suspension into the gelatin mold and releasing it from the mold at 37°C. The cell-related investigations indicate that the cells grow and spread well in the pure collagen vascular network scaffold. The proposed hybrid printing-then-casting approach also provides a feasible technology to fabricate with materials having low viscosity, long gelation time and poor mechanical property.

1. INTRODUCTION

Vascular networks, which deliver nutrients and oxygen to and remove metabolic byproducts from the organ systems, are of great significance and viewed as the first step to manufacture human tissues [1]. Typically, there are a few key components in a vascular network: the vascular lumen which functions as the source and sink for soluble and suspended factors, three-layered standalone vessels which may be integrated inside thick tissues or free standing, and/or extracellular matrix (ECM) which reside in the interstitial zone between standalone vessels. The

applications of vascular networks range from 3D cell culturing [2], to drug screening [3, 4], to tissue engineering [5, 6], to microfluidic devices for mixing [7] and biomimicry [8] and disease modeling [9].

Due to its excellent cyto-compatibility, pure collagen is the most abundant protein in mammalian bodies and has been one of the most promising biomaterials for tissue engineering applications [10-14]. It can provide mechanical support as well as control over cell adhesion and migration and tissue repair [15]. Moreover, collagen is the major stress-bearing component of the fibrous extracellular matrix of blood vessels due to its fibril-forming structure [16], and has the potential as the matrix material of the media layer of standalone vessels [17-19], which may be integrated inside thick tissues or free standing. Unfortunately, the viscosity of pure collagen is relatively low, preventing its wide applications in biofabrication-based tissue engineering, and no standalone vessel-based vascular networks/vascular network scaffolds have been reported thus far.

There are two main fabrication strategies investigated for the fabrication of vascular and vascular-like networks: sacrificial/porogen material-based fabrication and direct printing of network structures. For the sacrificial material-based approach, networked channels/lumens are usually created in bulk constructs (with or without living cells) using either embedded printing sacrificial rod-shaped tree patterns directly in bulk materials [20] (embedded printing, which can incorporate living cells into bulk materials as needed) or casting cell-laden materials over pre-formed (usually by printing) sacrificial scaffold patterns (printing-then-casting) [21-23]. Material extrusion [24] is usually the key printing technology to fabricate either rod tree patterns or scaffold patterns. After the two-dimensional (2D)/three-dimensional (3D) sacrificial patterns are fabricated and/or cast over, proper cross-linking stimuli are introduced to solidify the (cell-laden) hydrogel blocks which enclose them, resulting in the embedded sacrificial patterns in the gelled

(cell-laden) blocks. Then the sacrificial patterns are removed from the gelled constructs to create embedded vascular networks. Since extruded filaments are used directly to form 2D/3D sacrificial patterns, there are some constraints in adopting such a sacrificial material-based approach. Unfortunately, the vascular networks are part of the entire tissue construct as fabricated, and there is no standalone vessel structure distinguishable from neighboring ECM. Furthermore, the sacrificial material-based approach requires that the (cell-laden) matrix material should have the yield-stress property to effectively entrap rod tree patterns *in situ* during embedded printing or the sacrificial materials should have the rapid solidification property to retain the printed shape during printing-then-casting.

Alternatively, direct printing of vascular networks and/or vascular network scaffolds has been investigated as a free-form fabrication approach. During direct printing of cell-laden network structures, different 3D printing techniques have been adopted, such as inkjet printing [25-27], laser printing [28], and material extrusion [29-33]. Due to its high printing efficiency, wide range of applied materials and easy implementation, material extrusion has been widely utilized in 3D printing, in which ink materials are printed into complex 3D structures either in a support bath [30, 31] or directly in air [29, 33]. However, such extrusion-based freeform printing approach requires cell-laden bioinks either to have mechanical stiffness to be printed in and removed from yield-stress support bath [30, 31] or to have the rapid solidification property and self-supporting property to be directly printed in air [29, 33].

For collagen construct fabrication, usually other hydrogels with fast gelation rate, such as poly(ethylene glycol) diacrylate (PEGDA) [34] and alginate/gelatin blends [35], are mixed with collagen to facilitate 3D collagen structure fabrication. Thus far, pure or high-concentration collagen has not been explored to create 3D complex constructs, especially standalone vessels.

Neither the sacrificial material-based approach nor the direct printing approach works for the fabrication of pure collagen-based vascular structures. As aforementioned, the sacrificial material-based approach cannot create a standalone media layer of collagen. For the extrusion-based direct printing approach, since pure collagen constructs have weak mechanical properties [36, 37], they cannot be safely harvested from the yield-stress support bath after printing; since collagen-based bioink usually takes half an hour to three hours to solidify depending upon temperature conditions, it cannot be directly printed either.

Herein we propose a hybrid printing-then-casting approach to fabricate standalone collagen vessel-based vascular networks/vascular network scaffolds embedded with living cells, which can be further seeded with endothelial cells and cast over fibroblasts to make three-layered networks as needed. This hybrid approach combines the advantages of 3D printing such as customized design and manufacturing of freeform 3D complex vascular structures and the merits of casting which are not limited by the gelation rate and rheological property of collagen bioinks.

2. EXPERIMENTAL SECTION

2.1. Material preparation. Fugitive printing ink preparation. For the preparation of alginate-based fugitive ink, 6.0% (w/v) sodium alginate (NaAlg, Sigma-Aldrich, St. Louis, MO) was mixed with 3.0% (w/v) Laponite XLG (BYK Additives Inc., Gonzales, Texas) and 4.0% disodium hydrogen phosphate (Na_2HPO_4, Sigma-Aldrich, St. Louis, MO) by dispersing the 3appropriate amount of dry NaAlg, Laponite XLG and Na_2HPO_4 powders in deionized (DI) water at room temperature with continuous mixing. The mixing was performed by using an overhead stirrer (Thermo Fisher Scientific, Waltham, MA) at 500 rpm for a minimum of 60

minutes to ensure thorough hydration of the powders. To improve the visibility, Eosin Y disodium salt (Sigma-Aldrich, St. Louis, MO) was added to the prepared composite hydrogel suspension at a concentration of ~0.1% (w/v). Before printing, fugitive ink was degassed using a centrifuge (5804R, Eppendorf, Hamburg, Germany) at 2000 rpm for 5 minutes to remove entrapped bubbles.

In addition, 2.0%, 4.0%, 6.0% and 8.0% (w/v) NaAlg solutions were prepared for the investigation of the effects of alginate concentration on the mechanical property and diffusion and gelation time. Furthermore, Laponite XLG was mixed with 6.0% (w/v) NaAlg at concentrations of 1.0%, 2.0%, 3.0% and 4.0% (w/v) to determine the optimal mechanical property and rheological property, and Na_2HPO4 was mixed with 6.0% (w/v) NaAlg at concentrations of 1.0%, 2.0%, 3.0% and 4.0% (w/v) to determine the optimal diffusion and gelation time.

Support bath preparation. Laponite EP suspension-based support baths were prepared by dispersing the appropriate amount of dry Laponite EP powder in DI water at room temperature with continuous mixing for a minimum of 60 min to ensure thorough hydration of the Laponite solids. Laponite EP suspensions were stored in the dark in sealed containers to prevent degradation and evaporation and aged for one day. Calcium chloride ($CaCl_2$, Sigma-Aldrich, St. Louis, MO) was used as the cross-linking agent to cross-link sodium alginate structures in the Laponite EP bath. $CaCl_2$ solutions with concentrations of 0.25%, 0.50%, 1.00%, and 2.00% (w/v) were prepared by dispersing the appropriate amount of dry powder in DI water at room temperature with continuous mixing to investigate the effects of $CaCl_2$ concentration on the mechanical property and diffusion and gelation time. For printing applications, 4.0% (w/v) Laponite EP suspension with $CaCl_2$ (0.5% (w/v)) was prepared by mixing aged stock Laponite

EP (8.0% (w/v)) with aqueous 1.0% (w/v) $CaCl_2$ at 1:1 (v:v) and aged for at least one day before use.

Molding solution preparation. Gelatin (Type A, 300 bloom, from porcine skin, MP Biomedicals, Solon, OH) was used as the sacrificial molding solution and prepared by dispersing the appropriate amount of dry gelatin powder in 37ºC DI water with continuous mixing. Specifically, 5.0%, 10.0% and 15.0% (w/v) gelatin solutions were prepared to investigate the gelation time and mechanical property of gelatin at different concentrations. To improve the visibility, black, red, and blue food dyes (McCormick, Hunt Valley, MD) were added to the gelatin solutions with concentrations of 5.0%, 10.0%, and 15.0% (w/v), respectively .

Preparation of sodium citrate and collagen solutions. Sodium citrate ($Na_3C_6H_5O_7$, VWR, West Chester, PA) solution was used as the liquefaction agent to liquefy gelled alginate structures and was prepared by dispensing the appropriate amount of powder in DI water at room temperature with continuous mixing. Specifically, sodium citrate solutions with different molar concentrations (0.055, 0.110 and 0.220 mol/L) were prepared to test the liquefaction rate as well as the effects of sodium citrate concentration on the gelatin mold geometrical variation. Collagen (Type I, 8.56 mg/mL, Corning, NY), used as the casting solution, was prepared at the concentration of 3 mg/mL and neutralized per the manufacturer's protocol and stored in ice before use. In particular, the appropriate volume of phosphate buffered saline (PBS, 10×, MP Biomedicals, Solon, OH) was added into a sterile tube first. Then the appropriate volume of cold sodium hydroxide (NaOH, 1N, Sigma Aldrich, St. Louis, MO) solution was mixed with the PBS solution in the sterile tube. After that, the appropriate volume of DI water or cell-laden Dulbecco's Modified Eagles Medium (DMEM) (Sigma Aldrich, St. Louis, MO) suspension was added to the 10× PBS / 1N NaOH mixture. Finally, the appropriate volume of collage I was

mixed with the mixture in the sterile tube to make the neutralized collagen solution or cell-laden collagen suspension, respectively. The effect of NaOH concentration on the cell viability was not investigated herein, which is to be studied if it is of application concern.

2.2. Printing system and printing protocols. The extrusion-based 3D printing system was a micro-dispensing pump machine (nScrypt-3D-450, nScrypt, Orlando, FL), and all printing was conducted in ambient conditions. For alginate-based vascular tree pattern printing, a 25-gauge (250 μm inner diameter and 38.1 mm length) dispensing nozzle (EFD Nordson, Vilters, Switzerland) was used to deposit fugitive inks based on the designed path. The step distances along both the horizontal (*x*-) and vertical (*z*-) directions were set as 200 μm. The printing pressure was 1.38×10^5 Pa (20 psi), and the path speeds were 1.5 mm/s and 1.0 mm/s for vertical and branched section printing, respectively. After printing, the alginate-based vascular tree patterns were kept in the Laponite EP-Ca^{2+} bath for 24 hours for completely cross-linking and then taken out of the bath for residual Laponite rinsing as detailed in a previous study [31].

Digital 3D models for the various 2D patterns herein were designed using SolidWorks (Dassault Systemes SolidWorks Corp., Waltham, MA), and the codes and their instructions were manually programmed accordingly.

2.3. Rheological property measurement. Rheological properties of alginate-based fugitive inks were measured using a rheometer (Anton Paar MCR 92, Ashland, VA) with a cone-plate measurement geometry (a diameter of 50 mm, a cone-to-plate gap distance of 100 μm, and a cone angle of 1.00°). Frequency sweeps were performed by varying the frequency from 0.1 to 100 rad/s to investigate the effects of Laponite XLG on the fluid-like behavior of alginate-based fugitive inks, and the strain was controlled at 1.0%. Steady shear rate sweeps were conducted by varying the shear rate from 0.01 to 500 s^{-1} to determine the relationship between the viscosity and

shear rate of the 6.0% (w/v) NaAlg solution mixed with Laponite XLG at different concentrations.

2.4. Mechanical property measurement. Tensile test. A uniaxial tensile test was performed using a mechanical tester (eXpert 4000, Admet, Norwood, MA). Dogbone-shaped samples were fabricated by casting alginate-based solutions in a customized PDMS mold and cross-linked in a $CaCl_2$ bath for 12 hours. Then, tensile tests were performed at a strain rate of 1.0 mm/min and the stress-strain curve was determined based on the load and displacement data as well as the geometry of samples. The effective Young's modulus was calculated from the slope of the linear zone of the determined stress-strain curve. Specifically, samples made of different concentrated alginate solutions which were cross-linked by $CaCl_2$ at different concentrations were tested to investigate the effects of NaAlg and $CaCl_2$ concentrations on the mechanical properties. To investigate the effects of Laponite XLG on the mechanical properties, 6.0% (w/v) NaAlg mixed with different concentration Laponite XLG were cast and tested.

Compression test. Compression tests of gelatin samples at different concentrations were performed using the same eXpert 4000 mechanical tester at a strain rate of 1.0 mm/min. The cylindrical samples (Φ9.5 mm × 8.5 mm) were fabricated by casting in a customized PDMS mold and the stress-strain curve was determined based on the load and displacement data as well as the geometry of samples.

2.5. Diffusion and gelation time test. To mimic the diffusion and gelation process, alginate-based solutions were poured in a customized PDMS mold with a length of 20.0 mm, a width of 20.0 mm and a depth of 0.4 mm, and then submerged in a $CaCl_2$ bath to undergo a cross-linking process. The color and stiffness changes were used as the criteria to assess the gelation of the alginate-based solutions, and the time, at which the bottom of the sample changed its state from

liquid to solid, was recorded as the diffusion and gelation time. Specifically, the alginate samples at different concentrations were cross-linked in $CaCl_2$ baths of different concentrations to investigate the effects of concentration on the diffusion and gelation time. 6.0% (w/v) NaAlg mixed with Na_2HPO_4 at different concentrations were submerged in a 0.5% (w/v) $CaCl_2$ bath to assess the influence of Na_2HPO_4 as the cross-linking retardation agent.

2.6. Liquefaction test. Fugitive ink consisting of 6.0% (w/v) NaAlg, 3.0% (w/v) Laponite XLG and 4.0% (w/v) Na_2HPO_4 was poured in a customized PDMS mold (Φ9.5 mm × 5.0 mm) and cross-linked using 0.5% (w/v) $CaCl_2$. Then the gelled alginate-based samples were taken out of the PDMS mold and submerged in sodium citrate baths (10 mL) at different molar concentrations (0.055, 0.110, and 0.220 mol/L) and incubated on a shaker at room temperature. Liquefaction rate was determined by monitoring the mass loss over 4 hours, which was calculated as follows:

$$\text{Weight loss}=\left(\frac{M_0-M_f}{M_0}\right)\times 100$$

where M_0 was the initial mass of samples, and M_f was the final mass after each testing period.

2.7. Characterization of geometrical variation. 10% (w/v) gelatin samples (Φ9.5 mm × 5.0 mm) were prepared by casting in a customized PDMS mold and submerged in sodium citrate baths (10 mL) at different molar concentrations (0.055, 0.110, and 0.220 mol/L) for 2 days. The diameter and height of the samples were measured every 12 hours and the dimensional variation was calculated as follows:

$$\text{Dimensional change}=\left(\frac{D_0-D_f}{D_0}\right)\times 100$$

where D_0 was the initial diameter or height of the samples, and D_f was the final dimensions after each testing period.

2.8. Cell-laden collagen construct casting *and in vitro* cell studies. Suspended NIH-3T3 mouse fibroblasts (ATCC, Rockville, MD) were used to prepare cell-laden collagen suspensions. Specifically, the final cell density was 5×10^6 cells/mL for the morphology and cell viability test and 1×10^5 cells/mL for the metabolic activity test. The cell-laden collagen suspensions were neutralized per the manufacturer's protocol and then injected into the gelatin molds with a pipette. Then the injected gelatin molds were submerged in a Dulbecco's Modified Eagles Medium (DMEM) (Sigma Aldrich, St. Louis, MO) bath at room temperature (22°C) for 2 hours, and each collagen vascular network scaffold was cross-linked in the gelatin mold at the same time. Finally, the gelatin molds with the embedded collagen vascular network scaffold were submerged in a DMEM bath at 37°C to melt gelatin and release the cross-linked collagen constructs.

The cell-laden collagen networked constructs were cultured for 3 days in DMEM supplemented with 10.0% Fetal Bovine Serum (FBS) (HyClone, Logan, UT) in a humidified 5.0% CO_2 incubator at 37°C. The cell morphology of constructs on Day 0 and Day 3 was each examined by staining with fluorescein diacetate (FDA, Sigma, St. Louis, MO) at a final concentration of 10.0 μg/mL and Hoechst 33342 (Sigma Aldrich, St. Louis, MO) at a final concentration of 10.0 μg/mL, incubated in the dark for 5 minutes at room temperature, and imaged using the green fluorescent and blue fluorescent channels of a fluorescence microscope (EVOS FL, ThermoFisher Scientific, Waltham, MA) at 4× magnification.

For cell viability testing, the constructs were washed with 1.0× Phosphate Buffered Saline (PBS, Hyclone, Logan, Utah) for three times, and then digested with 0.1% Collagenase from

*Clostridium histolyticum (*Sigma Aldrich, St. Louis, MO) for 5 minutes, which was repeated three times to remove collagen completely and get the cell suspension. After that, 10 μL cell suspension was mixed with 10 μL of 0.4% trypan blue (Sigma Aldrich, St. Louis, MO) to test the cell viability. The cell viability was measured by counting live cells (unstained) and dead (stained, blue) cells in a hemacytometer with a transmitted-light microscope (EVOS XL, ThermoFisher Scientific, Waltham, MA). For metabolic activity testing, the cellular constructs were incubated for three days while the same volume cell-laden collagen suspension was kept as ungelled in a 96-well plate as a control group. The metabolic activity of the cells in the cast constructs and the control group was evaluated using the alamarBlue assay (Thermo Scientific, Rockford, IL) on Days 1, 2, and 3, respectively, per the manufacturer's protocol. The resulting fluorescence intensity was recorded using a fluorescence microplate reader (Synergy HT, Biotek, Winooski, VT).

2.9. Statistical analysis. All quantitative values of measurements in the figures were reported as mean ± one standard deviation (*SD*) with $n = 3$ samples per group. Statistical analysis was performed using analysis of variance (ANOVA) and p-values of less than 0.05 were considered statistically significant.

3. RESULTS AND DISCUSSION

3.1. Mechanism of hybrid printing-then-casting approach. This proposed hybrid fabrication approach includes 3D printing of fugitive alginate vascular tree patterns for molding and casting of collagen suspensions into a gelatin mold, which is made from fugitive alginate patterns. During extrusion-based 3D printing, a Laponite support bath-enabled fabrication

method [31] is utilized to fabricate a complex 3D vascular-like structure as the vascular tree pattern from a fugitive material. Herein, sodium alginate (NaAlg), a natural polysaccharide, is selected as the fugitive and reversible cross-linking material for its unique properties including its versatile functionality, gentle cross-linking kinetics, low cost, biocompatibility, low toxicity and environmental friendly nature [38]. The subsequent casting step consists of two sub-steps: 1) molding with a sacrificial molding material by embedding the printed alginate vascular-like tree pattern in the sacrificial material bath to make the mold. Gelatin, a natural hydrogel derived from collagen, is selected as the sacrificial molding material due to its biocompatibility, cross-linking reversibility, and recyclability; and 2) casting cell-laden collagen suspensions into the mold to make vascular constructs.

As shown in **Figure 1a-1**, a vascular tree pattern is first printed in a Laponite EP-calcium chloride ($CaCl_2$) bath using a NaAlg solution. Laponite EP is selected as the support bath material since its pH value close to neutral and can be readily used for bioprinting [31, 32]. In addition, organic modification has been performed during Laponite EP preparation which can reduce its ionic sensitivity, enabling Laponite EP miscible with some ionic solutions while retaining its original rheological properties [31]. Thus, calcium cations (Ca^{2+}) can be mixed with Laponite EP to cross-link the printed alginate structure in the Laponite EP bath. When the *α-L*-guluronic acid (G units/blocks) of NaAlg interacts with calcium cations in the support bath, calcium cations form interchain ionic bonds between G blocks, resulting in a stable calcium alginate network as shown in **Figure 1a-2**. To ensure the mechanical property of the printed vascular tree pattern, both the concentrations of NaAlg and $CaCl_2$ solutions are optimized for a stable "printing-then-solidification" process as described in the previous studies [31]. After cross-linking, the solidified vascular tree pattern is harvested from the Laponite bath and submerged in

a gelatin bath at 37ºC in order to form a gelatin mold with an embedded calcium alginate pattern as shown in **Figure 1b-1**. By decreasing the temperature of the gelatin bath to room temperature, some segments (e.g. repeating amino acid sequence glycine-proline-hydroxyproline) in the gelatin molecular chains adopt the triple helical conformation, forming junctions between gelatin molecules. This results in a calcium alginate tree pattern-embedded bulk gelatin mold as shown in **Figure 1b-2**. Then, the bulk gelatin mold is submerged in a sodium citrate bath as shown in **Figure 1c-1**. With the help of sodium citrate, the solidified calcium alginate tree pattern is liquefied as shown in **Figure 1c-2**. After removing the liquefied residual alginate solution from the solidified gelatin, a gelatin mold with an annular vascular channel is fabricated as shown in **Figure 1c-3**. Finally, a neutralized cell-laden collagen precursor suspension is poured into the gelatin mold at room temperature as shown in **Figure 1d-1**. Collagen molecules are comprised of three parallel polypeptides (α-chains) which coil around with each other to form a right-handed triple-helical chain. Under different conditions, collagen can be cross-linked either chemically or physically [39]. Herein, sodium hydroxide (NaOH) is used as the cross-linking agent to adjust the pH value of the collagen precursor to around 7, enlist the amino and carboxyl groups on collagen molecular chains to form new covalent bonds and finally solidify the cast collagen vascular construct at room temperature (**Figure 1d-2**). By increasing the temperature to 37ºC, the triple helical conformation of gelatin molecules is disentangled (**Figure 1d-3**), and the gelatin mold melts and releases the solidified cell-laden collagen vascular construct as shown in **Figure 1d-2**.

3.2. Design of alginate-based fugitive inks. The design of alginate-based fugitive inks for pattern making during "printing-then-solidification" and subsequent molding is critical for the proposed hybrid approach to be successful. An ideal fugitive ink should satisfy the following criteria: the resulting pattern should be strong enough to survive the post-printing

rinsing/cleaning process, the fugitive ink should have good printability, and the solidification process is easily tunable during pattern making.

Strong vascular tree pattern is critical for the subsequent molding process. After cross-linking, the alginate-based pattern needs to be taken out of the Laponite bath, and some post-treatments are needed to rinse residual Laponite EP suspensions away from the surface and lumen of the printed vascular tree pattern. Thus, the mechanical strength which is needed to ensure the pattern integrity during the post-treatment rinsing process is adopted as a criterion to determine the formula of fugitive inks. For the evaluation of the mechanical strength of alginate-based vascular tree patterns during the Laponite rinsing process, a simplified mechanics model is used based on the schematic shown in **Figure 2a**. Using Lame's equation, the radial stress (σ_r) and hoop stress (σ_θ) can be calculated as $\sigma_r = \frac{r_i^2 P_i - r_o^2 P_o}{r_o^2 - r_i^2} - \frac{(P_i - P_o) r_i^2 r_o^2}{(r_o^2 - r_i^2) r^2}$ and $\sigma_\theta = \frac{r_i^2 P_i - r_o^2 P_o}{r_o^2 - r_i^2} + \frac{(P_i - P_o) r_i^2 r_o^2}{(r_o^2 - r_i^2) r^2}$, respectively, where r_i is the inner radius, r_o is the outer radius, P_i is the inner pressure, P_o is the outer pressure, and r is the radius measured from the center. Based on the dimensions of the vascular tree pattern and the zero-shear-rate viscosity of the Laponite EP suspension (**Figure S1**), the maximum stress in the vascular tree pattern during rinsing is the hoop stress (200 kPa) at the inner surface of the lumen ($r=r_i$) as detailed in **Supporting Information S1**. For a tree pattern to survive during rinsing, it should have a fracture strength higher than 200 kPa.

Since alginate is the functional component of fugitive inks in this study, the effect of NaAlg and $CaCl_2$ concentration on the mechanical strength is investigated. It is noted that the mechanical strength of 3D printed parts depends on the mechanical strength of each layer and the interfacial strength between adjacent layers. Different concentration combinations of NaAlg and $CaCl_2$ solutions are studied first to obtain a relatively high mechanical strengths of each cross-

linked layer as shown in **Figures S2** and **S3** (**Supporting Information**). To ensure the interfacial strength of the vascular tree pattern, the "printing-then-solidification" procedure is utilized, in which printed layers are at liquid state and fuse well with each other during printing [31]. Thus, the diffusion and gelation rate of alginate gelled with $CaCl_2$ at different concentrations are investigated as shown in **Supporting Information S4**. The results are summarized as a phase diagram illustrated in **Figure 2b**. As seen from **Figure 2b**, it is found that 6.0% (w/v) alginate and 0.5% (w/v) $CaCl_2$ can be potentially used as the main component of the fugitive ink and the cross-linking agent, respectively. Under this condition the cross-linked vascular tree pattern has a fracture strength of approximately 85 kPa (lower than the theoretical fracture strength of 200 kPa) and a cross-linking duration of approximately 4.5 minutes determined based on the casting of 0.5 mm thick alginate sheet, which is shorter than the printing time of 35 minutes in this study. Although the strategy of increasing NaAlg concentration while decreasing $CaCl_2$ concentration can also improve the mechanical property and slow the gelation rate of the alginate-based fugitive ink, such an adjustment may affect the printability of the fugitive ink and the efficiency of liquefying high-concentration alginate structures. Thus, an alternative strategy needs to be explored.

Since the alginate-only fugitive ink doesn't result in a strong enough tree pattern to survive the post-treatment handling and rinsing process, Laponite XLG is added in to enhance the mechanical strength of the alginate tree pattern. Besides being a support bath material, Laponite can be used as a physical cross-linker to improve the mechanical properties of hydrogel composites and is widely utilized in tissue engineering [40-42]. Herein, biocompatible Laponite XLG, one of the most common Laponite products [40-42], is selected to mix with the alginate solution and further enhance its mechanical properties. When mixing with alginate, gel

composites are formed by physical bonding, including hydrogen bonding as well as van der Waals and ionic interactions between Laponite nanosilicate fillers and the alginate molecular network [43-45]. Such high surface interaction between alginate molecular chains and the anisotropic, plate-like and higher aspect-ratio morphology of the Laponite nanosilicates results in an increase of the mechanical properties of the alginate-Laponite composite. Accordingly, the effects of Laponite XLG concentration on the mechanical properties of alginate samples are studied, and the Young's modulus and fracture strength are measured as shown in **Figure 2c**. As seen from **Figure 2c**, the addition of Laponite XLG leads to a significant increase in the Young's modulus and fracture strength, and the mechanical properties increase when the Laponite XLG concentration increases. Specifically, the increase of fracture strength ranges from 1.6-fold to 3.5-fold when the Laponite XLG concentration increases from 1.0% to 4.0% (w/v). Considering the maximum hoop stress (approximately 200 kPa) in the post-treatment process, 3.0% (w/v) is selected as the final concentration of additive Laponite XLG, under which the fracture strength of the alginate-Laponite XLG hydrogel composite is approximately 250 kPa, higher than the maximum hoop stress.

In addition, Laponite XLG behaves as a rheological additive to enhance the printability of alginate-based fugitive inks. The effect of Laponite XLG concentration on the viscosity is tested by steady shear rate sweeps, and its results are shown in **Figure 2d**. With the increase of Laponite XLG concentration, the viscosity increases, indicating that the extrudability of alginate-Laponite hydrogel precursor composites with a higher Laponite concentration is better than those with a lower Laponite concentration. In addition, the effect of Laponite XLG concentration on the shear moduli is investigated using oscillatory frequency sweeps, and the results are illustrated in **Figure S5** (**Supporting Information**). As seen from **Figure S5**, it is found that the loss

modulus of the pure alginate solution is higher than the storage modulus which verifies that the alginate solution without Laponite XLG presents liquid-like property. After mixing with Laponite XLG, both storage and loss moduli of alginate-Laponite hydrogel precursor composites increase, and at lower frequencies the storage modulus is higher than the loss modulus, resulting in a solid-like state of hydrogel precursor composites.

Furthermore, disodium hydrogen phosphate (Na_2HPO_4) is added into the alginate-based fugitive inks too as a cross-linking retardation agent to tune the solidification process of the alginate-based fugitive inks. When the ink composed of alginate and Na_2HPO_4 is extruded in the Laponite-Ca^{2+} bath, Na_2HPO_4 reacts with Ca^{2+} firstly ($CaCl_2+Na_2HPO_4 \rightarrow CaHPO_4+NaCl$) as the cross-linking retardation step, and then the Ca^{2+} cations are slowly released to react with alginate chains to form an egg-box structure and finally become the gel state (alginate cross-linking step). By varying the Na_2HPO_4 concentration, the diffusion and gelation time of the mixed fugitive inks are measured as shown in **Figure 2e**. With the increase of Na_2HPO_4 concentration, the diffusion and gelation time of alginate-based inks increases significantly. For verification, vertical tubes are fabricated using the alginate-based inks with different Na_2HPO_4 concentrations, and the resulting tubes can be seen in the insets of **Figure 2e**. At the lower Na_2HPO_4 concentration (1.0% (w/v)), the outside surface of alginate-based filaments solidifies quickly during printing. As a result, the subsequently deposited filament cannot fuse well with the previous one, leading to the poor interfacial strength and further resulting in an aggregate of continuous filaments after rinsing the residual Laponite. By increasing the Na_2HPO_4 concentration, the alginate gelation rate decreases gradually. Thus, the tube morphology changes from a surface with pronounced interfacial lines (2.0% (w/v)) to a smooth surface (3.0% and 4.0%

(w/v)). As a result, 4.0% (w/v) is determined as the final Na_2HPO_4 concentration for the cross-linking retardation purpose during pattern printing.

As such, the fugitive ink is optimized as follows for the printing of vascular-like patterns in the Laponite EP-Ca^{2+} bath: 6.0% (w/v) alginate, 3.0% (w/v) Laponite XLG and 4.0% (w/v) Na_2HPO_4. While the formula of the fugitive ink was determined based on the dimensions of the vascular-like patterns in this study, the methodology to design fugitive inks can be applied to optimize the composition of similar fugitive inks for broad applications of vascular network fabrication. To evaluate the printing quality of alginate-based structures fabricated using the proposed fugitive ink, a liquid filament is deposited in the Laponite EP bath without undergoing solidification, and the effects of aqueous diffusion on the filament diameter and morphology during the following 60 minutes are recorded as shown in **Figure S6** (**Supporting Information**). As seen from **Figure S6** and its insets, the filament has the well-defined geometry and a relatively smooth surface which is attributed to the nanoscale of Laponite EP particles as the support bath material. While keep in the Laponite bath, the filament diameter only increases slightly (from approximately 288 μm to 312 μm) during the observation period. That is because the addition of Laponite XLG can physically cross-link with alginate molecular chains in addition to the ionic cross-linking of alginate with Ca^{2+} cations. From application wise, such a dual cross-linking mechanism can effectively help maintain the deposited filament shape for a long time and mitigate the effect of aqueous diffusion.

3.3. Investigation of molding materials. Besides the design of alginate-based fugitive inks for pattern printing, molding material should also receive special attention. An ideal molding material should have a proper solidification time to construct a mold with sufficient strength and be easily removed after molding. Reversibly thermosensitive and biocompatible gelatin is

selected as the molding material. Gelatin is derived from collagen and widely used for biological applications, and its gelation time is a function of its concentration. Since the molding process is performed at room temperature, the gelation rate of gelatin bath may affect its implementation significantly, and the gelation time needs to be long enough to avoid early gelation of the gelatin bath. As a result, the gelation time of gelatin at different concentrations is measured at room temperature and shown in **Figure 3a**. As seen from **Figure 3a**, it is found that with the increase of concentration, the gelation time decreases significantly. After removing the alginate-based vascular tree pattern in the solidified gelatin, the gelatin core (**Figure 1c-3**) must be self-supporting to form a gelatin mold with well-defined geometry. As a result, it is also necessary to evaluate the mechanical properties of gelatin at different concentrations. Considering the stress condition in gelatin mold, uniaxial compression tests are performed herein, and the compression modulus and fracture strength are measured and shown in **Figure 3b** and **Figure S7** (**Supporting Information**). From **Figure 3a** and **b**, we find that the higher concentration gelatin (e.g. 15% (w/v)) has much better mechanical properties but a shorter gelation time, while the lower concentration gelatin (e.g. 5% (w/v)) has a longer gelation time but poor mechanical properties. As such, we use 10% (w/v) gelatin to make the mold due to its acceptable mechanical properties and suitable gelation rate.

3.4. Investigation of liquefaction agents. After the gelatin molding process is complete, pattern removal is accomplished by using sodium citrate to liquefy the alginate pattern to make a gelatin mold with networked annual channels. First, the effect of sodium citrate concentration on the liquefaction rate is investigated by monitoring the weight loss of the mold samples made by the proposed alginate-based fugitive ink, and the result is illustrated in **Figure 3c**. As seen from **Figure 3c**, it is found that sodium citrate solutions with higher molar concentration lead to the

rapid liquefaction of alginate-based structures. However, the geometry of gelatin molds may also be affected by sodium citrate during alginate liquefaction. As such, the geometry variations including the radial and axial geometrical changes of cylindrical gelatin samples are investigated as a function of the molar concentration of sodium citrate, and the result is shown in **Figure 3d**. As seen from **Figure 3d**, it is found that gelatin samples swell in sodium citrate baths and the higher sodium citrate concentration results in the relatively smaller geometrical variation. Such gelatin swelling is caused by the water diffusion into the gelatin sample which is driven by the osmotic pressure. Based on the Morse equation, the osmotic pressure (Π) can be predicted by $\Pi=RTC$, where R is the gas constant, T is the thermodynamic temperature and C is the water molar concentration. In sodium citrate solutions with higher molar concentration, C is relatively low which leads to a lower osmotic pressure. Since the water cannot easily diffuse into the gelatin sample, the resulting geometrical variation of the gelatin sample is relatively small. By considering both the liquefaction rate and geometrical variation, we use 0.220 mol/L sodium citrate to liquefy the alginate pattern in the solidified gelatin molds.

3.5. Fugitive vascular pattern printing and gelatin mold fabrication. Based on the aforementioned fabrication knowledge, cell-laden standalone collagen vascular network scaffolds are further fabricated. First, a vascular tree pattern is printed in the Laponite EP-Ca^{2+} bath using the fugitive ink as shown in **Figure 4a** and **Movie M1** (**Supporting Information**). During printing, the interfacial overlap (or the step size in the printing directions) of two adjacent layers affects their interfacial strength. During branched section printing, the interfacial overlap between adjacent layers (**Figure S8c** of **Supporting Information**) is smaller than that during vertical section printing (**Figure S8b** of **Supporting Information**) due to the given step distance along the z direction. To address this challenge, the filament diameter should vary during the

printing of different sections to ensure the desirable interfacial overlap (**Figure S8d** of **Supporting Information**). Since the diameter of extruded filaments is a function of operating conditions as well as rheological properties of both the support bath and liquid build material [32], herein the effect of path speed (one of the main operating conditions) on the filament diameter is measured (**Figure S8e** of **Supporting Information**). Two different path speeds (v_{p1} and v_{p2}) are utilized to print the vertical and branched sections of the vascular tree patterns, respectively under which the interfacial overlap between adjacent filaments can be a constant as shown in **Figure S8f** (**Supporting Information**). After solidification in the Laponite bath, the gelled vascular tree pattern is harvested from the bath, and the residual Laponite on the surface and in the lumen is rinsed by pipetting DI water through the lumen in a DI water bath as shown in **Movie M2** (**Supporting Information**). The Laponite-free vascular tree pattern and its lumen morphology are imaged as shown in **Figure 4b** and its insets. To further prove that the residual Laponite in the network lumen is completely removed, DI water with red dye is pipetted through the lumen as shown in **Figure 4c** and **Movie M3** (**Supporting Information**). Finally, a comparison between the 3D model and 3D printed vascular tree pattern is included in **Figure S9** (**Supporting Information**) to demonstrate the print fidelity of the alginate-based pattern printed in the Laponite EP bath.

Then, the alginate-based vascular tree pattern is submerged in a gelatin bath at 37 °C and embedded to form a vascular pattern-encapsulated gelatin mold at room temperature as shown in **Figure 4d**. One end of the vascular pattern-encapsulated gelatin mold is cut open as the sodium citrate inlet to liquefy the alginate-based pattern and to expose the annular channels as shown in the insets of **Figure 4d**. After submerging the mold in a sodium citrate bath for two days as shown in **Figure 4e**, the alginate-based pattern is gradually liquefied, and the gelatin mold with

the annular channels is fabricated by pipetting out the liquefied pattern as shown in **Figure 4e-1**. DI water with red dye can be pipetted into the annular channels to check whether the alginate-based pattern is completely liquefied or not, as seen in **Figure 4e-2** by visually comparing with the design of the vascular tree pattern.

3.6. Standalone cell-laden collagen vascular network scaffold casting and cell-related investigation. Finally, cell-laden collagen suspension is injected in the gelatin mold by carefully pipetting to uniformly fill the annular channels, resulting in the standalone cell-laden collagen vascular network scaffold. The neutralized collagen solution is gradually cross-linked at room temperature. To avoid unnecessary evaporation of the cell-laden collagen suspension during cross-linking, the filled gelatin mold is submerged in a Dulbecco's Modified Eagles Medium (DMEM) bath as shown in **Figure 5a**. After chemical cross-linking in the gelatin mold, the standalone cell-laden collagen vascular network scaffold is released from the gelatin mold by submerging in a DMEM bath at 37 °C as shown in **Figure 5b**. The resulting standalone vascular network scaffold can be seen in **Figure 5c** and its inset. To verify the vascular network scaffold with the lumens, two cross sections (one in the branched section and another in the vertical section) along the vascular network scaffold are selected, cut, and imaged using microscopy, and the results are shown in **Figure 5c-2** and **c-3**. The wall thicknesses of the branched and vertical sections are measured as 0.81 mm and 0.92 mm, respectively, which verifies the uniformity of the wall thickness across the collagen vascular network scaffold. The wall thicknesses are close to the designed value of 0.80 mm. In addition, the dimensions of the collagen vascular network scaffold are measured and shown in **Figure S10** (**Supporting Information**) to demonstrate the dimensional fidelity of the proposed hybrid fabrication approach. Cell viability and spreading in the collagen vascular network scaffold is investigated as shown in **Figure 5d**. After releasing

from the gelatin mold, fluorescent dyes are used to mark all the cells and living cells in the collagen vascular network scaffold as shown in **Figure 5d-1**. As seen from **Figure 5d-1**, most of the cells are alive in the collagen vascular network scaffold. After three-day incubation, the cells spread and proliferate as shown in **Figure 5d-2** and its inset. To prove the cell-compatibility of the proposed fabrication approach, 3-day cell viability is tested and illustrated in **Figure 5e**. The cell viability is higher than 90% after the 3-day incubation. Since the cell-laden collagen construct is fabricated by casting instead of extrusion printing, the shear stress-induced cell damage [46] commonly occurring in extrusion can be effectively mitigated, resulting in the relatively high cell viability [47]. Finally, the metabolic activity of cultured cells in the collagen vascular network scaffold is investigated by monitoring alamarBlue reduction after 1, 2, and 3 days, and the result is shown in **Figure 5f**. The cells in the collagen vascular network scaffold grow well and proliferate during the 3-day incubation period, indicating the excellent bioprinting feasibility of the proposed hybrid printing-then-casting approach.

4. CONCLUSIONS

In summary, we propose a hybrid printing-then-casting approach to fabricate standalone cell-laden collagen vascular networks/vascular network scaffolds. The Laponite support bath-enabled 3D printing approach is used to fabricate the vascular tree pattern in the support bath. The alginate-based fugitive ink with the excellent mechanical strength (by adding Laponite), printability (by adding Laponite), and controllable gelation rate (by adding disodium hydrogen phosphate) is investigated, which can further be used to print other complex structures as patterns in the Laponite support bath. In addition, the gelation time and mechanical properties of gelatin as the thermally reversible molding material are studied. Moreover, the effect of sodium

citrate on the liquefaction rate and geometrical variation is systemically investigated to effectively remove the alginate-based pattern and fabricate the vascular pattern-encapsulated gelatin mold. Finally, the standalone cell-laden collagen vascular network scaffolds are successfully fabricated using the proposed hybrid approach. The 3T3 fibroblast-based cell-related investigations indicate that the cells grow and spread well in the pure collagen vascular network scaffolds, and in the future human smooth muscle cells will be used to fabricate standalone cellular vascular networks. It is noted that the fabrication of 3D complex structures using difficult-to-print materials, which are defined as liquid materials with low viscosity, long gelation time and poor mechanical property, is always a challenge for conventional 3D printing techniques. The proposed hybrid approach provides a feasible technology to fabricate such difficult-to-print materials. While the fabricated vascular networks only have one cellular layer (as the media), other cells can be seeded to be the intima layer and cast over the standalone collagen networks to be the adventitia layer, resulting in three-layered vascular constructs to mimic blood vessels in the future. It is noted that the dimensional limitations of vascular networks/vascular network scaffolds, such as the minimum lumen diameter, wall thickness, and size of vascular networks/vascular network scaffolds, fabricated by the proposed hybrid approach are influenced by different factors including the minimum filament diameter, mechanical property of vascular networks/vascular network scaffolds, feasibility of removing residual Laponite from vascular tree patterns, and feasibility of injecting cell-laden collagen suspensions in gelatin molds, to name a few. For this study, the collagen vascular network scaffolds have been designed and fabricated with a wall thickness of 0.80 mm based on the diffusion limitation from both sides, which has been proven feasible with the material selection and fabrication protocol herein. Future work should study the achievable dimension range during

vascular network/vascular network scaffold fabrication based on the realistic blood vessel anatomy, available materials, and printing conditions during vascular network/vascular network scaffold fabrication.

ACKNOWLEDGEMENTS

This research was partially supported by NSF (CMMI-1762941), and the access of the Anton Paar rheometer at the University of Florida is appreciated.

SUPPORTING INFORMATION

Supporting Information is available free of charge from the ACS Applied Materials & Interfaces home page (http://pubs.acs.org/journal/aamick).

Supporting Information S1: Evaluation of stress distribution in the vascular tree pattern during Laponite rinsing. (PDF)

Supporting Information S2: Tensile testing of alginate samples. (PDF)

Supporting Information S3: Mechanical properties of alginate samples. (PDF)

Supporting Information S4: Determination of diffusion and gelation time of alginate samples. (PDF)

Supporting Information S5: Effects of Laponite XLG on the rheological property of alginate-based fugitive inks. (PDF)

Supporting Information S6: Characterization of deposited alginate-based filaments in Laponite EP bath. (PDF)

Supporting Information S7: Compression testing. (PDF)

Supporting Information S8: Investigation of the effect of interfacial overlap. (PDF)

Supporting Information S9: Evaluation of printed fugitive vascular tree patterns. (PDF)

Supporting Information S10: Evaluation of fabricated collagen vascular network scaffolds. (PDF)

Supporting Information M1: Alginate-based vascular tree pattern printing in Laponite bath. (Movie)

Supporting Information M2: Residual Laponite rinsing from a vascular tree pattern. (Movie)

Supporting Information M3: Lumen testing in a vascular tree pattern. (Movie)

AUTHOR CONTRIBUTIONS

Y.J. and Y.H. conceived the concept of this work, Y.J. conducted the printing experiments and analysis, W.C. performed the biological testing, and Y.J. and Y.H. wrote the manuscript.

COMPETING FINANCIAL INTERESTS

There are no competing financial interests.

REFERENCES

1. Huang, Y.; Schmid, S. R. Additive Manufacturing for Health: State of the Art, Gaps and Needs, and Recommendations. *Journal of Manufacturing Science and Engineering* **2018,** DOI: 10.1115/1.4040430.

2. Pampaloni, F.; Reynaud, E. G.; Stelzer, E. H. The Third Dimension Bridges the Gap between Cell Culture and Live Tissue. *Nature Reviews Molecular Cell Biology* **2007,** *8*, 839-845.

3. Huh, D.; Hamilton, G. A.; Ingber, D. E. From 3D Cell Culture to Organs-On-Chips. *Trends in cell biology* **2011,** *21*, 745-754.

4. Bhatia, S. N.; Ingber, D. E. Microfluidic Organs-on-Chips. *Nature Biotechnology* **2014,** *32*, 760-772.

5. Langer, R.; Vacanti, J. P. Tissue Engineering. *Science* **1993,** *260,* 920-926.

6. Murphy, S. V.; Atala, A. 3D Bioprinting of Tissues and Organs. *Nature Biotechnology* **2014,** *32*, 773-785.

7. Therriault, D.; White, S. R.; Lewis, J. A. Chaotic Mixing in Three-Dimensional Microvascular Networks Fabricated by Direct-Write Assembly. *Nature Materials* **2003,** *2*, 265-271.

8. Wheeler, T. D.; Stroock, A. D. The Transpiration of Water at Negative Pressures in a Synthetic Tree. *Nature* **2008,** *455*, 208-212.

9. Lee, G. Y.; Kenny, P. A.; Lee, E. H.; Bissell, M. J. Three-Dimensional Culture Models of Normal and Malignant Breast Epithelial Cells. *Nature Methods* **2007,** *4*, 359-365.

10. Harkness, R. D. Biological Functions of Collagen. *Biological Reviews* **1961,** *36*, 399-455.

11. Chevallay, B.; Herbage, D. Collagen-Based Biomaterials as 3D Scaffold for Cell Cultures: Applications for Tissue Engineering and Gene Therapy. *Medical and Biological Engineering and Computing* **2000,** *38,* 211-218.

12. Tan, H.; Marra, K. G. Injectable, Biodegradable Hydrogels for Tissue Engineering Applications. *Materials* **2010,** *3*, 1746-1767.

13. Parenteau-Bareil, R.; Gauvin, R.; Berthod, F. Collagen-Based Biomaterials for Tissue Engineering Applications. *Materials* **2010,** *3,* 1863-1887.

14. Paten, J. A.; Siadat, S. M.; Susilo, M. E.; Ismail, E. N.; Stoner, J. L.; Rothstein, J. P.; Ruberti, J. W. Flow-Induced Crystallization of Collagen: a Potentially Critical Mechanism in Early Tissue Formation. *ACS Nano* **2016,** *10,* 5027-5040.

15. Kadler, K. E.; Baldock, C.; Bella, J.; Boot-Handford, R. P. Collagens at a Glance. *Journal of Cell Science* **2007,** *120,* 1955-1958.

16. Voet, D.; Voet, J. G. Three-Dimensional Structures of Proteins-Fibrous Proteins-Collagen. *Biochemistry* **2004,** 233-239.

17. Boccafoschi, F.; Habermehl, J.; Vesentini, S.; Mantovani, D. Biological Performances of Collagen-Based Scaffolds for Vascular Tissue Engineering. *Biomaterials* **2005,** *26,* 7410-7417.

18. Boccafoschi, F.; Rajan, N.; Habermehl, J.; Mantovani, D. Preparation and Characterization of a Scaffold for Vascular Tissue Engineering by Direct-Assembling of Collagen and Cells in a Cylindrical Geometry. *Macromolecular Bioscience* **2007,** *7,* 719-726.

19. Price, G. M.; Wong, K. H.; Truslow, J. G.; Leung, A. D.; Acharya, C.; Tien, J. Effect of Mechanical Factors on the Function of Engineered Human Blood Microvessels in Microfluidic Collagen Gels. *Biomaterials* **2010,** *31,* 6182-6189.

20. Wu, W.; DeConinck, A.; Lewis, J. A. Omnidirectional Printing of 3D Microvascular Networks. *Advanced Materials* **2011,** *23,* 178-183.

21. Miller, J. S.; Stevens, K. R.; Yang, M. T.; Baker, B. M.; Nguyen, D. H. T.; Cohen, D. M.; Chaturvedi, R. Rapid Casting of Patterned Vascular Networks for Perfusable Engineered Three-Dimensional Tissues. *Nature Materials* **2012,** *11,* 768-774.

22. Kolesky, D. B.; Truby, R. L.; Gladman, A.; Busbee, T. A.; Homan, K. A.; Lewis, J. A. 3D Bioprinting of Vascularized, Heterogeneous Cell-Laden Tissue Constructs. *Advanced Materials* **2014,** *26*, 3124-3130.

23. Kolesky, D. B.; Homan, K. A.; Skylar-Scott, M. A.; Lewis, J. A. Three-Dimensional Bioprinting of Thick Vascularized Tissues. *Proceedings of the National Academy of Sciences* **2016,** *113*, 3179-3184.

24. Huang, Y.; Leu, M. C.; Mazumder, J.; Donmez, A. Additive Manufacturing: Current State, Future Potential, Gaps and Needs, and Recommendations. *Journal of Manufacturing Science and Engineering* **2015,** *137,* 014001.

25. Nishiyama, Y.; Nakamura, M.; Henmi, C.; Yamaguchi, K.; Mochizuki, S.; Nakagawa, H.; Takiura, K. Development of a Three-Dimensional Bioprinter: Construction of Cell Supporting Structures Using Hydrogel and State-of-the-Art Inkjet Technology. *Journal of Biomechanical Engineering* **2009,** *131,* 035001.

26. Xu, C.; Chai, W.; Huang, Y.; Markwald, R. R. Scaffold-Free Inkjet Printing of Three-Dimensional Zigzag Cellular Tubes. *Biotechnology and Bioengineering* **2012,** *109,* 3152-3160.

27. Christensen, K.; Xu, C.; Chai, W.; Zhang, Z.; Fu, J.; Huang, Y. Freeform Inkjet Printing of Cellular Structures with Bifurcations. *Biotechnology and Bioengineering* **2015,** *112,* 1047-1055.

28. Xiong, R.; Zhang, Z.; Chai, W.; Huang, Y.; Chrisey, D. B. Freeform Drop-on-Demand Laser Printing of 3D Alginate and Cellular Constructs. *Biofabrication* **2015,** *7,* 045011.

29. Kucukgul, C.; Ozler, S. B.; Inci, I.; Karakas, E.; Irmak, S.; Gozuacik, D.; Taralp, A.; Koc, B. 3D Bioprinting of Biomimetic Aortic Vascular Constructs with Self-Supporting Cells. *Biotechnology and Bioengineering* **2015,** *112,* 811-821.

30. Jin, Y.; Compaan, A. M.; Bhattacharjee, T.; Huang, Y. Granular Gel Support-Enabled Extrusion of Three-Dimensional Alginate and Cellular Structures. *Biofabrication* **2016,** *8,* 025016.

31. Jin, Y.; Compaan, A. M.; Chai, W.; Huang, Y. Functional Nanoclay Suspension for Printing-then-Solidification of Liquid Materials. *ACS Applied Materials & Interfaces* **2017,** *9,* 20057-20066.

32. Jin, Y.; Chai, W.; Huang, Y. Printability Study of Hydrogel Solution Extrusion in Nanoclay Yield-Stress Bath during Printing-Then-Gelation Biofabrication. *Materials Science and Engineering C* **2017,** *80,* 313-325.

33. Ahlfeld, T.; Cidonio, G.; Kilian, D.; Duin, S.; Akkineni, A. R.; Dawson, J. I.; Gelinsky, M. Development of a Clay Based Bioink for 3D Cell Printing for Skeletal Application. *Biofabrication* **2017,** *9,* 034103.

34. Hockaday, L. A.; Kang, K. H.; Colangelo, N. W.; Cheung, P. Y. C.; Duan, B.; Malone, E.; Chu, C. C. Rapid 3D Printing of Anatomically Accurate and Mechanically Heterogeneous Aortic Valve Hydrogel Scaffolds. *Biofabrication* **2012,** *4,* 035005.

35. Wu, Z.; Su, X.; Xu, Y.; Kong, B.; Sun, W.; Mi, S. Bioprinting Three-Dimensional Cell-Laden Tissue Constructs with Controllable Degradation. *Scientific Reports* **2016,** *6,* 24474.

36. Wallace, D. G.; Rosenblatt, J. Collagen Gel Systems for Sustained Delivery and Tissue Engineering. *Advanced Drug Delivery Reviews* **2003,** *55,* 1631-1649.

37. Helary, C.; Bataille, I.; Abed, A.; Illoul, C.; Anglo, A.; Louedec, L.; Giraud-Guille, M. M. Concentrated Collagen Hydrogels as Dermal Substitutes. *Biomaterials* **2010,** *31,* 481-490.

38. Luginbuehl, V.; Wenk, E.; Koch, A.; Gander, B.; Merkle, H. P.; Meinel, L. Insulin-like Growth Factor I-Releasing Alginate-Tricalciumphosphate Composites for Bone Regeneration. *Pharmaceutical Research* **2005,** *22,* 940-950.

39. Chattopadhyay, S.; Raines, R. T. Review Collagen-Based Biomaterials for Wound Healing. *Biopolymers* **2014,** *101*, 821-833.

40. Xavier, J. R.; Thakur, T.; Desai, P.; Jaiswal, M. K.; Sears, N.; Cosgriff-Hernandez, E.; Gaharwar, A. K. Bioactive Nanoengineered Hydrogels for Bone Tissue Engineering: a Growth-Factor-Free Approach. *ACS Nano* **2015,** *9,* 3109-3118.

41. Hong, S.; Sycks, D.; Chan, H. F.; Lin, S.; Lopez, G. P.; Guilak, F.; Zhao, X. 3D Printing of Highly Stretchable and Tough Hydrogels into Complex, Cellularized Structures. *Advanced Materials* **2015,** *27,* 4035-4040.

42. Jin, Y.; Liu, C.; Chai, W.; Compaan, A.; Huang, Y. Self-Supporting Nanoclay as Internal Scaffold Material for Direct Printing of Soft Hydrogel Composite Structures in Air. *ACS Applied Materials & Interfaces* **2017,** *9,* 17456-17465.

43. Loizou, E.; Butler, P.; Porcar, L.; Kesselman, E.; Talmon, Y.; Dundigalla, A.; Schmidt, G. Large Scale Structures in Nanocomposite Hydrogels. *Macromolecules* **2005,** *38,* 2047-2049.

44. Loizou, E.; Butler, P.; Porcar, L.; Schmidt, G. Dynamic Responses in Nanocomposite Hydrogels. *Macromolecules* **2006,** *39,* 1614-1619.

45. Schexnailder, P.; Schmidt, G. Nanocomposite Polymer Hydrogels. *Colloid and Polymer Science* **2009,** *287,* 1-11.

46. Nair, K.; Gandhi, M.; Khalil, S.; Yan, K. C.; Marcolongo, M.; Barbee, K.; Sun, W. Characterization of Cell Viability during Bioprinting Processes. *Biotechnology Journal* **2009,** *4,* 1168-1177.

47. Yin, J.; Yan, M.; Wang, Y.; Fu, J.; Suo, H. 3D Bioprinting of Low-Concentration Cell-Laden Gelatin Methacrylate (GelMA) Bioinks with a Two-Step Cross-linking Strategy. *ACS applied materials & interfaces* **2018,** *10*, 6849-6857.

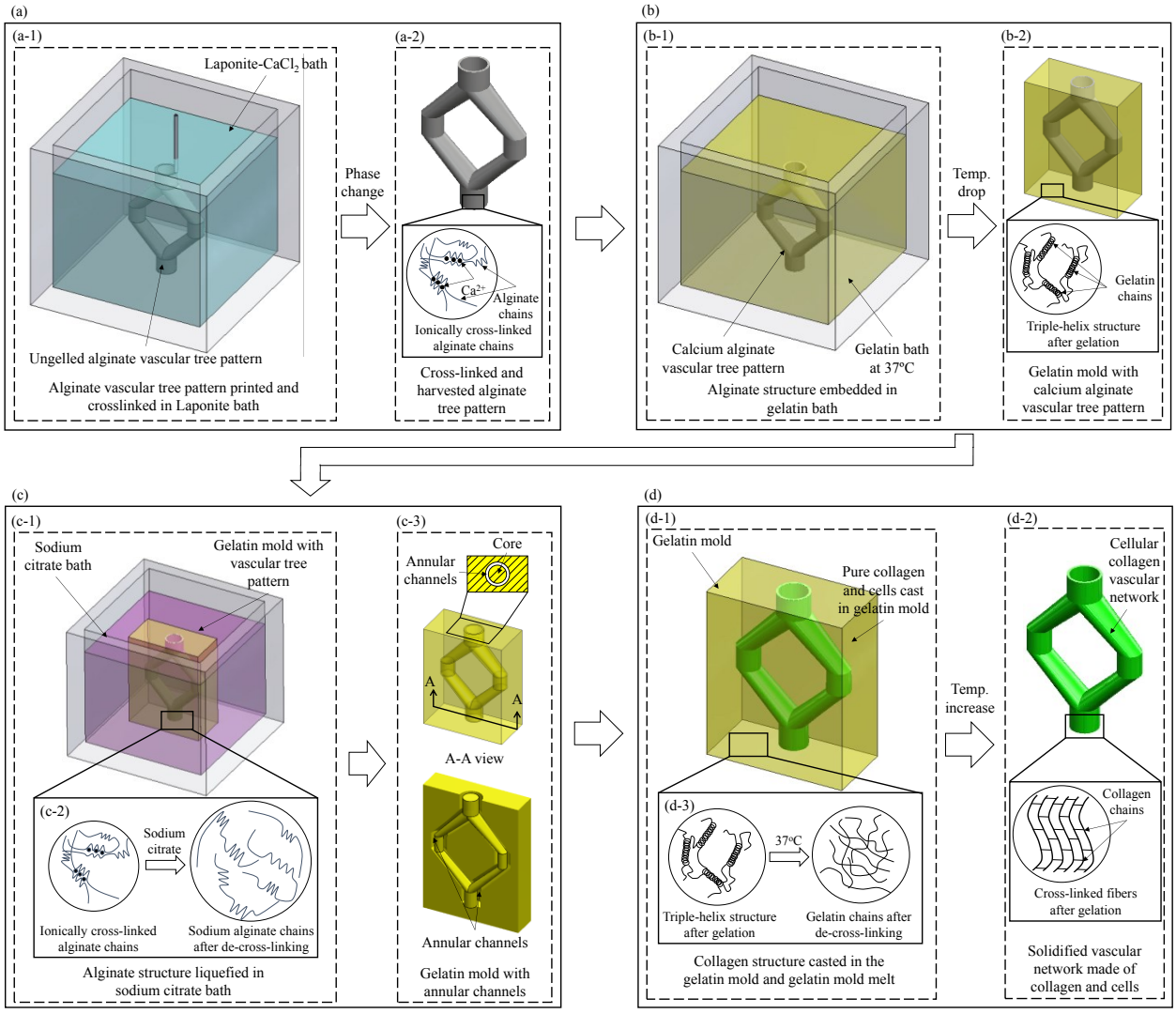

Figure 1. Schematic of hybrid printing-then-casting approach. a) Alginate vascular tree pattern printing in Laponite EP-calcium chloride bath. Molding: b1) embedding calcium alginate vascular tree pattern in liquid gelatin bath and b2) gelatin gelation. c) Gelatin mold fabrication with annular channels using sodium citrate. d) Vascular or vascular-like collagen construct fabrication by casting collagen precursor in gelatin mold and harvesting by melting gelatin mold at higher temperature.

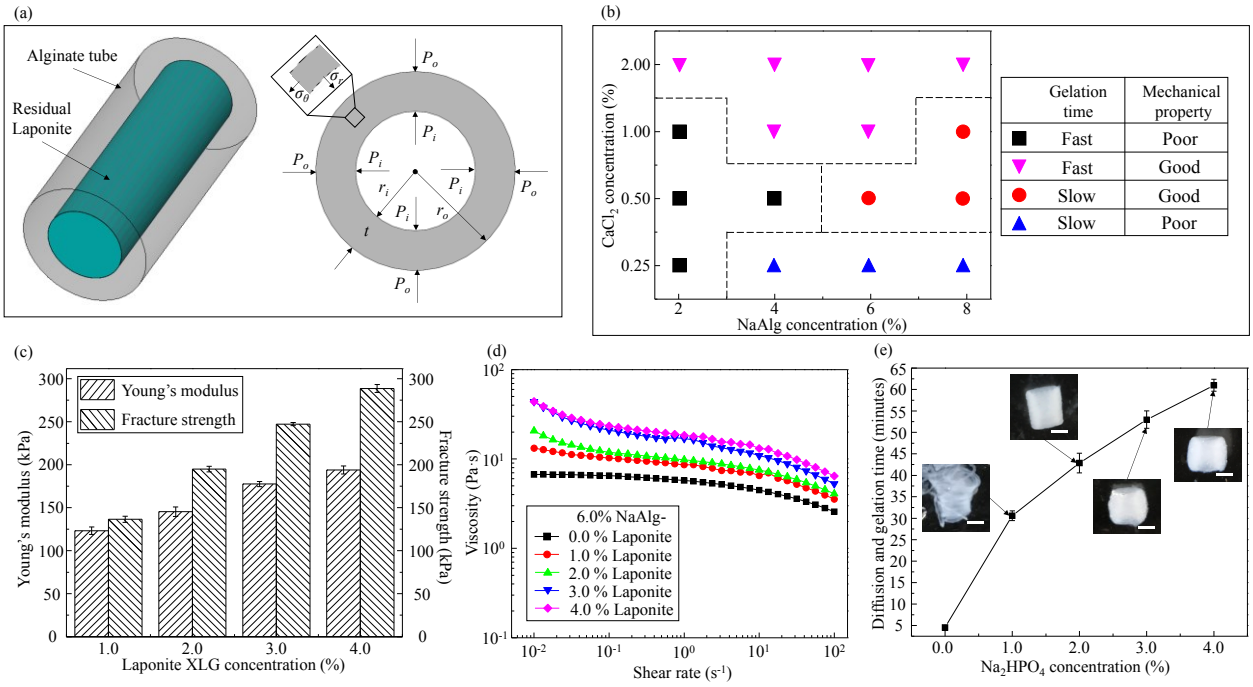

Figure 2. Design of alginate-based fugitive inks. a) Stress analysis in thick-walled tube. b) Phase Diagram for concentration selection of NaAlg and $CaCl_2$ solutions. c) Effects of Laponite XLG concentration on the mechanical properties of alginate-based vascular tree patterns. d) Effects of Laponite XLG concentration on the viscosity of alginate-based fugitive inks. e) Effects of Na_2HPO_4 concentration on the diffusion and gelation time of alginate-based fugitive inks. (Scale bars: 2.0 mm, and error bars: plus/minus one sigma)

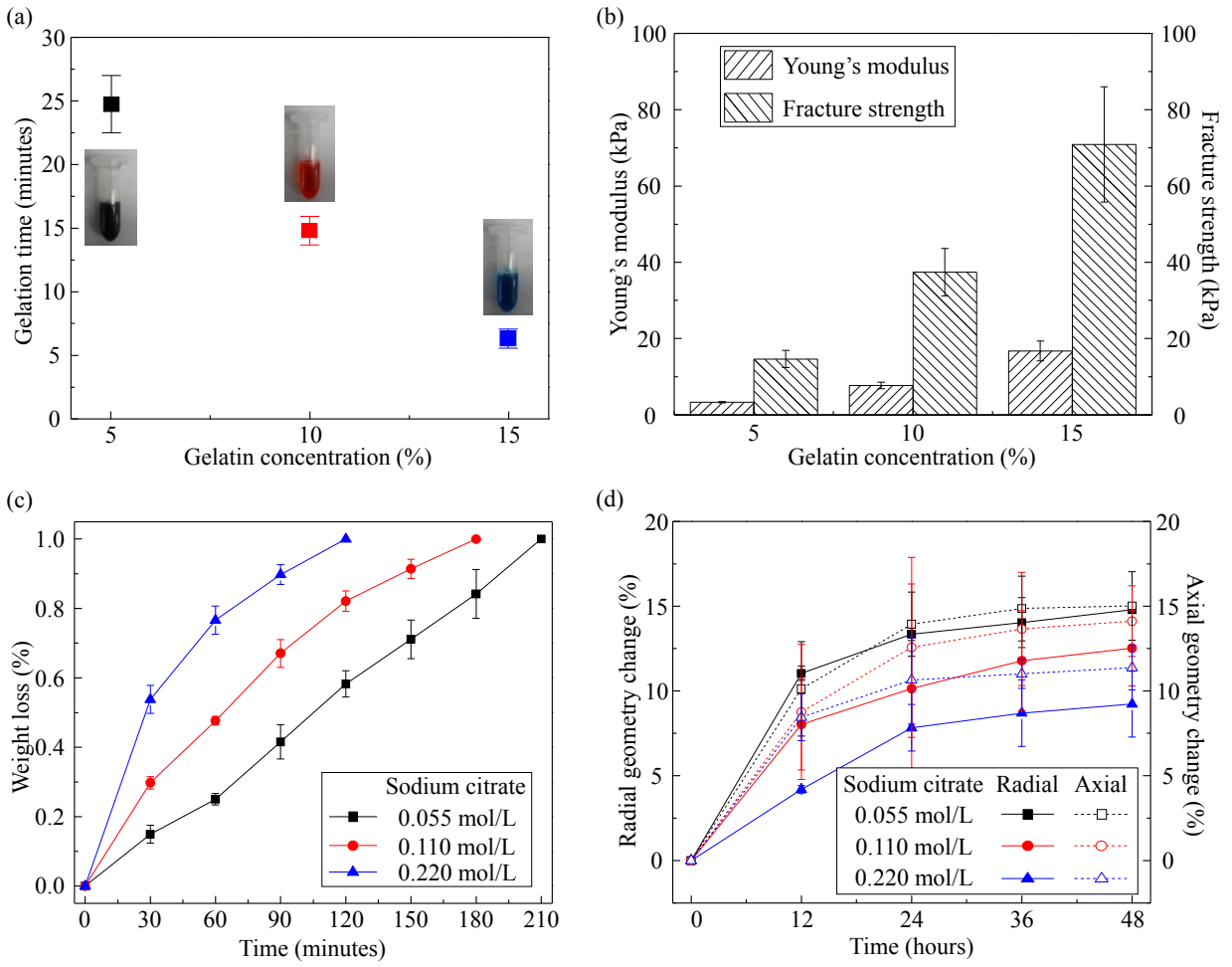

Figure 3. Characterization of gelatin as molding material and sodium citrate as liquefaction agent. a) Gelation time as a function of gelatin concentration. b) Mechanical properties as a function of gelatin concentration. c) Liquefaction rate as a function of submerging time in sodium citrate bath with different molar concentrations. d) Radial and axial geometry variation of gelatin samples in sodium citrate bath with different molar concentrations. (Error bars: plus/minus one sigma)

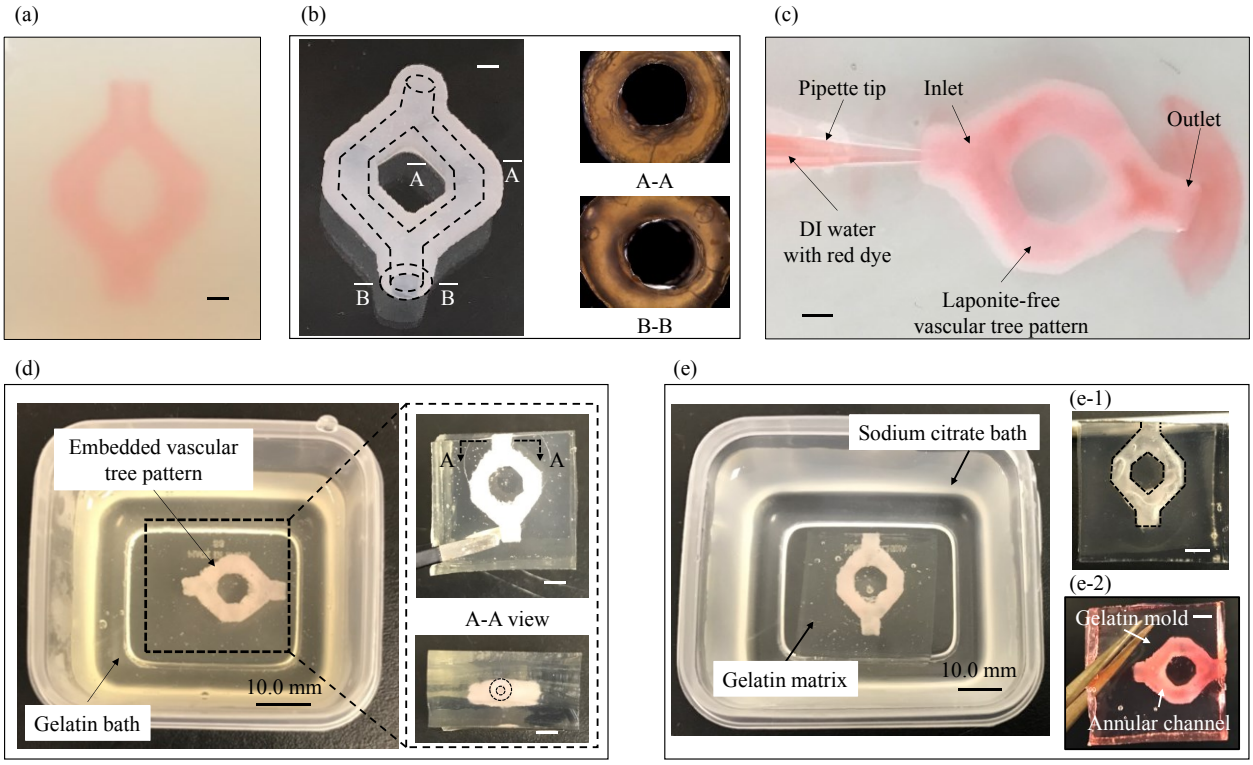

Figure 4. Printing of vascular tree pattern and fabrication of gelatin mold. a) Alginate-based vascular tree pattern printing in Laponite EP-Ca2+ bath. b) Gelled Laponite-free alginate-based vascular tree pattern after collecting from Laponite EP bath and rinsing residual Laponite on surface and in lumen. c) Pattern testing by pipetting DI water with red dye. d) Gelatin molding using alginate-based vascular tree pattern. e) Alginate-based vascular tree pattern liquefaction in sodium citrate bath and resultant gelatin mold with annular channels e-1) and e-2). (Scale bars: 2.0 mm for a) b) and c) and 4.0 mm for d) and e))

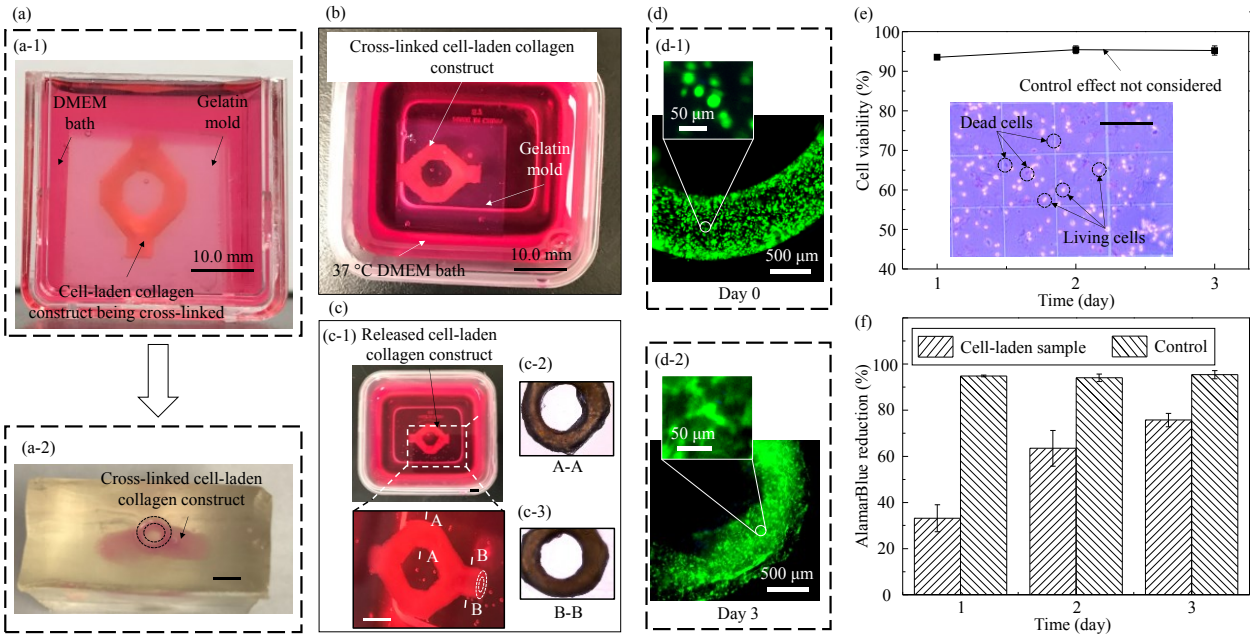

Figure 5. Standalone cell-laden pure collagen vascular network scaffold fabrication and cell-related investigation. a) Neutralized cell-laden collagen suspension cross-linking in gelatin mold. b) Cross-linked cell-laden collagen vascular network scaffold releasing from gelatin mold in DMEM bath at 37 °C. c) Released standalone cell-laden collagen vascular network scaffold and its cross-section images (c-2) branched section and c-3) vertical section). d) Fluorescent images at d-1) Day 0 and d-2) Day 3. e) Cell viability after 3-day incubation. f) Metabolic activity of cultured cells in collagen vascular network scaffold. (Error bars: plus/minus one sigma)

Table of Contents Graph

A fugitive vascular tree pattern-based printing-then-casting approach is proposed and investigated to fabricate standalone cell-laden collagen vascular networks/vascular network scaffolds. Patterns for molding are printed using an alginate-based fugitive ink which has good printability and a tunable cross-linking rate and results in patterns with good mechanical strength. Standalone cell-laden collagen vascular network scaffold can be fabricated by casting cell-laden collagen suspension into a gelatin mold, which is molded using printed fugitive patterns, and releasing it from the mold at 37°C.